Journal of Asian Earth Sciences 133 (2017) 12–23

Contents lists available at ScienceDirect

Journal of Asian Earth Sciences

journal homepage: www.elsevier.com/locate/jseaes

Characteristic ground motions of the 25th April 2015 Nepal earthquake (Mw 7.9) and its implications for the structural design codes for the border areas of India to Nepal

Babita Sharma *, Prasanta Chingtham, Varun Sharma, Vikas Kumar, H.S. Mandal, O.P. Mishra

National Centre for Seismology, Ministry of Earth Sciences, New Delhi 110003, India

ARTICLE INFO

Article history:
Received 3 November 2015
Received in revised form 2 June 2016
Accepted 12 July 2016
Available online 25 July 2016

Keywords:
Geo-morphological constraints
BIS-2002 codes
Earthquake risk resilient
Response
Alluvium

ABSTRACT

The 25th April 2015 Nepal Earthquake was found associated with a series of aftershocks, and the mainshock rupture propagated predominantly towards SE direction where a major aftershock (Mw 7.3) rocked on 12th May 2015 to the east of the mainshock that enhanced the rate of occurrence of aftershocks in the affected region. We conducted a rigorous analysis of strong motion data to understand the characteristics of ground motion and their bearing on the structural design codes, responsible for the damage to the structures in the border area of India to Nepal. The effect of ground geology on the acceleration response spectra are also evaluated using main shock and its associated strong earthquakes. All the sites used in the present analysis are located on alluvium deposits showing a predominant period of 0.242 sec for horizontal components and at 0.193 sec for vertical components. Our results demonstrated that observed Peak Ground Acceleration (PGA) has prominent distribution in the border cities of UP and Bihar. PGA ranges from 3 to 80 cm/sec^2 in the study region for the epicentral distance varying from 120 km to 495 km with respect to the source zone (mainshock). The Peak Ground Velocity (PGV) varies from 1 to 16 cm/sec while the Peak Ground Displacement (PGD) lies in between 1 cm and 20 cm for the same area. Our study shows that variation of PGD, PGV, and PGA are controlled and dictated by the geomorphological constraints, besides the nature and extent of structural heterogeneities of the subsurface geological formation materials. The obtained normalised spectral amplifications are compared with the Bureau of Indian Standard code for construction of buildings which shows that the current Indian building design code is within the structural limits proposed for the seismic forces at all periods for alluvium sites, suggesting that the structural heterogeneity has the strong role contributing towards the intrinsic attenuation in the seismic wave propagating medium. Our analysis also shows a good correspondence with the nonlinearity of the seismic waves, which in turn controls the degree of damage in an area. We infer that extent of damage to the structures in the border cities of India, vicinity to the rupture zone can be avoided if the existing building design code could have been implemented as the earthquake risk resilient mitigation plan.

1. Introduction

A major earthquake (Mw 7.9) occurred in the central Nepal region on 25th April 2015 at 11:41 h (IST) at a depth of 15 km, which was located 281 km north of Patna, Bihar and about 120 km NNE of Bagha, Uttar Pradesh (UP) of India. The 25th April 2015 Nepal mainshock (28.1°N, 84.6°E) occurred in the expected seismic gap zone of the central Himalayan region, which has complex seismotectonic settings. It is, therefore the occurrence of the mainshock was not a puzzle since the continued accumulation of strain energy in the intricate seismic gap zone with significant structural heterogeneities may have initiated the brittle failure beneath the central Himalaya (Mishra, 2014a,b). It has been observed that the rupture of Nepal earthquake propagated in the south-east direction from the epicentre towards Kathmandu city, potentially leading to more severe destruction in Kathmandu. The rapid loss estimation of CATDAT gives a total damage value coming out to between 3 and 3.5 billion USD. The 2nd triggered earthquake has caused much additional damage (Cedim report, 2015). According to USGS report the intensity in Kathmandu was IX, which is considered to be violent. Tremors were also felt widely in the neighbouring Indian states of Bihar, Uttar Pradesh, Assam, West Bengal, Sikkim, Uttarakhand, Odisha, Andhra Pradesh,

* Corresponding author.
E-mail address: babita_s@rediffmail.com (B. Sharma).

http://dx.doi.org/10.1016/j.jseaes.2016.07.021
1367-9120/

Gujarat, Delhi and Karnataka as well. Many buildings were damaged in Bihar, where the intensity was between VI and VII. Geologically, this earthquake is located in Lesser Himalayan domain, bounded on the north by Main Central Thrust (MCT) across which Higher Himalayan crystalline override southward (Fig. 1). The main features named as the Main Central Thrust (MCT), the Main Boundary Thrust (MBT) and the Himalayan Frontal Thrust (HFT) of the Nepal Himalaya has experienced slip due to the thrust nature of these faults (Gansser, 1964; DeCelles et al., 2001; Robinson et al., 2003; http://geode.colorado.edu/~sheehan/pdf/MonsalveJGR08.pdf). The complex seismotectonic setting of the central Nepal Himalaya is very intriguing and complicated. The MHT (Main Himalayan Thrust) exhibits a ramp-flat geometry with a dip of 15° for a ramp that begins nearly 70 km north of the HFT (Herman et al., 2010). Along the Himalayan arc, MHT also displays lateral variations in terms of geometry (Robert et al., 2011). In between the MBT and MCT, there exists the Lesser Himalayan thrust belt that has experienced multiple phases of contraction (Schelling and Arita, 1991). That is why continued crustal deformation in the central Himalayan region further complicates the pattern of seismogenesis beneath the region. The crustal deformation occurs mostly on the MHT (Cattin and Avouac, 2000) where the Indian lithosphere underthrusts beneath this region (Zhao et al., 1993; Nakata, 1989). That explains the occurrence of intense microseismicity due to the stress accumulation at the downdip edge of the locked fault resulting in a seismic belt, which underlies a zone of greater stress accumulation rate along the front of the high range in Nepal Himalaya (Pandey et al., 1995, 1999). In review of the seismotectonic set up in light of abovementioned intricate earthquake generating environment, it is observed that the mainshock was confined to the Gorkha district of the central Nepal that ruptured a large, gently dipping thrust fault in Central Himalaya and had occurred about 200 km west of the 1934 Bihar Nepal earthquake (M 8.2). The focal depth of this event is in the range 15 km coupled with strike 295° paralleling the geology low-angle northeast dip of 7° (CMT Harward) is consistent with the seismotectonic model, which indicates that hypocenters of great and major earthquakes in the lesser Himalaya are confined to the locked section of the detachment (Seeber et al., 1981; Ni and Barazangi, 1984). Here it is worthwhile to mention about the Central Seismic Gap (CSG) extending from 1905 Kangra Earthquake (Mw 7.8) to 1934 Bihar Nepal Earthquake (M 8.2) and has the potential to generate a great earthquake as described by Khattri (1999). The CSG is also studied by several researchers and they argued that the zone has potential to generate earthquakes because of continuous strain building (Khattri, 1987; Khattri and Tyagi, 1983; Rajendran et al., 2015). Fig. 1 shows the schematic representation of the Nepal Earthquakes (Mw 7.9 and Mw 7.3) and the corresponding aftershock sequence up to 30th September 2015. Mostly the sequence of aftershocks is

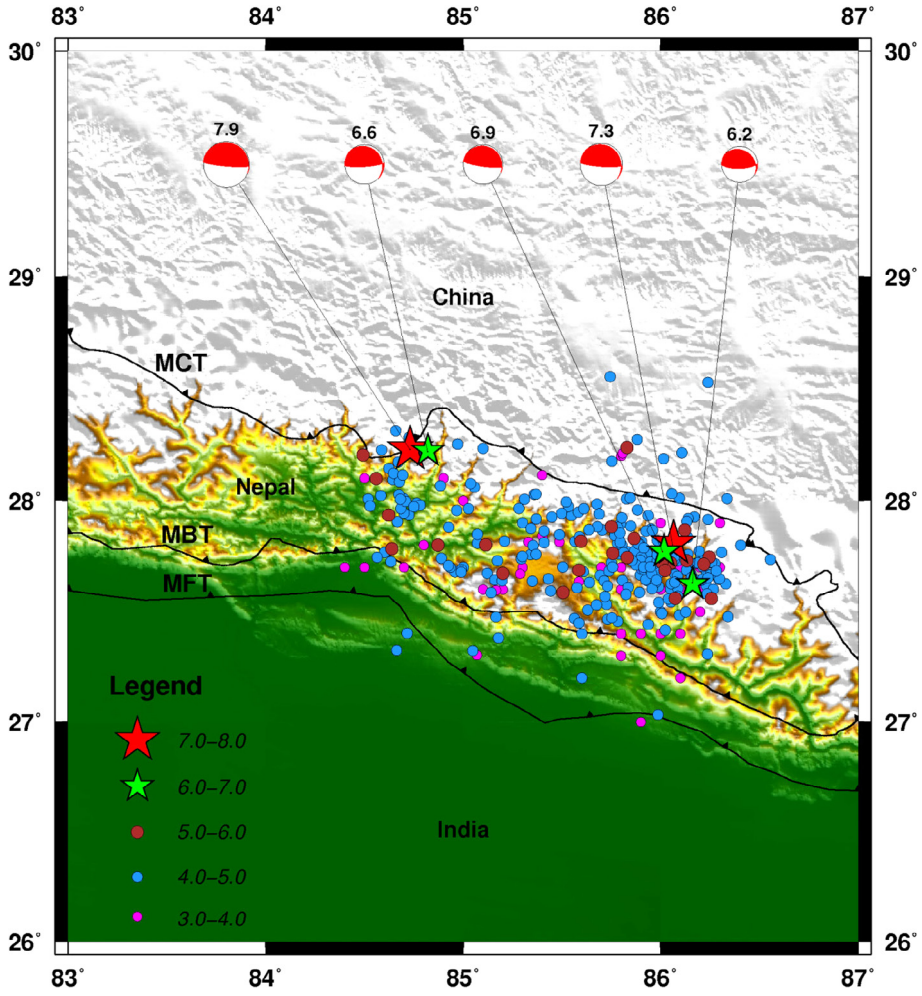

Fig. 1. Nepal Earthquakes (Mw 7.9) and (Mw 7.3) given by red star, strong aftershocks shown by green stars and related aftershock sequence up to 30th September 2015. Fault plane solutions for earthquakes plotted here are taken from CMT Harward. Magnitudes of main-shock and it strong aftershocks are taken from India Meteorological Department (IMD). (For interpretation of the references to colour in this figure legend, the reader is referred to the web version of this article.)

conspicuously found concentrated in the SE direction to the mainshock that corresponds to the mainshock rupture direction.

The maximum slip in Nepal earthquake, estimated from slip models, observed for Nepal earthquake is around 5 m (Mitra et al., 2015) by shifting Kathmandu nearly 3 m to the south in 30 sec. The mainshock in Nepal initiated an eastward-propagating fault rupture which pushed an oval-shaped segment of the Himalaya of size approximately 150 km long and 65 km wide southward over the Indian Plate (Bilham, 2015). Slip model of Nepal earthquake generated by Wang and Fialko, 2015 suggested that the Nepal earthquake ruptured a deeper part of the seismogenic zone in the Main Frontal Thrust of Himalaya while in the case of 1934 Bihar Nepal earthquake the shallower part of the adjacent fault was ruptured. Galetzka et al. (2015) found slip pulse and resonance of Kathmandu basin during Nepal earthquake. Yagi and Okuwaki (2015) assessed the acceleration and deceleration of dynamic rupture for the 2015 Nepal earthquake. Several other researchers also analyzed seismo-geodetic, InSAR and ALOS data to estimate slip rate and the rupture directivity of the 2015 Nepal earthquake (Avouac et al., 2015; Denolle et al., 2015; Parameswaran et al., 2015; Galetzka et al., 2015; Fan and Shearer, 2015; Feng et al., 2015; Lindsey et al., 2015). However, there is no study made for the 2015 Nepal earthquake to understand the detailed impact of strong motion on the geo-mechanical properties of the sub-surface formations and its inter-relationship with damage potential of the shaking. It is worthwhile to mention that the extent of ground acceleration due to great/big earthquake has a close bearing on the sub-surface rock material heterogeneities as well with the geo-mechanical strength of the sub-surface soil formations that may get affected differently under varying frequency of the earthquake shaking. Also the attenuation of seismic waves plays an important role which is the cause of the dissipating the energy of the wave into the medium which has been verified by several studies in India and worldwide (Aki and Chouet, 1975; Sharma et al., 2015; Sharma, 2014; Sharma and Rastogi, 2014). In this study, we analyzed strong motion records recorded by a total of 13-strong motion stations ascribed to the Ministry of Earth Science, New Delhi, India, which were installed in different parts of Uttarpradesh and Bihar, the border states of India with Nepal to understand the characteristics of ground motion and their bearing on the structural design codes. This endeavour may provide a plausible explanation for the degree of damage to the structures in the earthquake affected region. We attempted to estimate different parameters, such as PGA, PGV, and PGD and their distribution with respect to distance. The effect of ground geology on the acceleration response spectra are also evaluated using the mainshock and its associated strong aftershocks. The normalised response spectra have been compared with BIS code (2002) for the seismic forces applicable in the entire country India.

2. Data and analysis

The strong motion Accelerograph (SMA) network installed by IIT, Roorkee and funded by Ministry of Earth Sciences covers the entire Himalayan range from Jammu & Kashmir to Meghalaya. In the present study, strong motion data of sites located in Uttar Pradesh and Bihar states of India from this network has been used (Fig. 2). These instruments are installed at various locations of varied geological conditions in the entire Himalayan range (Mittal et al., 2006; Kumar et al., 2012). Table 1 depicts the details of stations whose data have been used in the present analyses. The SMA's consist of an internal AC-63 GeoSIG triaxial force-balanced accelerometers and GSR-18 GeoSIG 18-bit digitizers with external GPS. The recording for all instruments is in trigger mode at a sampling frequency of 200 sps. All the data used in the present analysis has been base line corrected and also the band pass filtered from 0.01 to 25 Hz. This base line corrected and filtered data has been used to find the PGA, PGV, PGD and response in the area of study.

Accelerogram is integrated once to estimate velocity while it is integrated twice to calculate displacement. The maximum value obtained for acceleration, velocity and displacement are assigned PGA, PGV and PGD respectively. We applied Duhamel Integral approach to generate the acceleration response spectra of each record at every site using components consisted of two horizontal and one vertical. The geometric mean of the two horizontal acceleration response spectra of each record at each station is

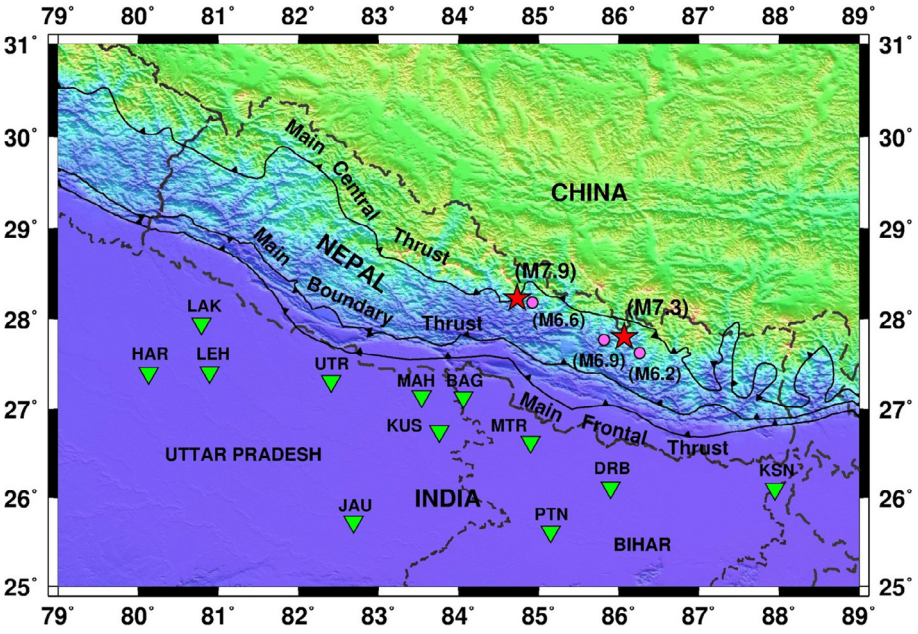

Fig. 2. Plot of stations in eastern Uttar Pradesh and northern Bihar (Inverted green triangles) where the data of SMA network related to earthquakes of (Mw 7.9 on 25-04-2015, Mw 6.6 on 25-04-2015, Mw 6.9 on 26-04-2015 and Mw 7.3 on 12th May) have been recorded. (For interpretation of the references to colour in this figure legend, the reader is referred to the web version of this article.)

Table 1
Locations of the SMA stations deployed in the states of Eastern Uttar Pradesh and Northern Bihar of India.

S. no.	Station code	Station name	Station latitude	Station longitude	State
1	LAK	Lakimpur Kheri	27.95	80.79	Uttar Pradesh
2	MAH	Maharaj Ganj	27.14	83.54	Uttar Pradesh
3	TUL	Tulsipur	27.53	82.40	Uttar Pradesh
4	UTR	Utraula	27.31	82.41	Uttar Pradesh
5	KUS	KushiNagar	26.75	83.76	Uttar Pradesh
6	LEH	Laharpur	27.41	80.89	Uttar Pradesh
7	JAU	Jaunpur	25.73	82.69	Bihar
8	DRB	Darbhanga	26.12	85.90	Bihar
9	HAR	Hardoi	27.40	80.13	Bihar
10	PTN	Patna	25.62	85.15	Bihar
11	BAG	Bagha	27.13	84.06	Bihar
12	MTR	Motihari	26.63	84.90	Bihar
13	KSN	Kishanganj	26.10	87.95	Bihar

determined. The mean and mean plus sigma are estimated to get average acceleration response spectra for each component of the recoded stations. The spectra are normalised to get normalised spectral acceleration (SA) with the first value of ground acceleration. The stations with the same geology are grouped together and weighted average acceleration response spectra for particular geological formation in the study area are determined. The weighted average is considered due to the fact that different numbers of records are available at each recording site. Our used stations are mostly located in the area of Indo-Gangetic plain associated with quaternary sediments. Fig. 3 presents the subsurface geology and tectonic framework of the upper and middle Ganga basin along with the stations used in the present study (Sinha et al., 2005). Such type of SMA data is very important as it can be used to simulate the strong ground motions for the worst case scenarios for future probable big/great earthquakes in the corresponding regions in order to be used further for new constructions & retrofitting the existing structures accordingly (Sharma et al., 2013, 2015, 2016). In present study SMA stations deployed in UP and Bihar states of India are used to study characteristic ground motion and average response spectra, by averaging the response spectra for each site in the study area.

3. Results and discussions

In the present study, the effect of ground geology on the acceleration response spectra is evaluated at sites situated in Uttar Pradesh and Bihar states of India. For this purpose, Nepal Earthquake (Mw 7.9) of 25th April 2015 and its associated aftershocks (Mw 6.6 & 6.9) along with an earthquake occurred on 12th May 2015 (Mw 7.3) have been used for the analysis. Peak Ground Acceleration (PGA) ranges from 3 to 80 cm/sec^2 for the distance varying from 120 km to 495 km from the source of the Nepal earthquakes as shown in Fig. 4 and Tables 2a and 2b; whereas Fig. 5a shows PGA distribution with respect to distance from mainshock and its two aftershocks along with the shock of 12th May 2015. We attempted to compare the distribution of PGA calculated for different distances for the mainshock (Mw 7.9) using the attenuation relationship developed by Sharma et al. (2009) for Himalayan earthquakes. It is observed that the PGA for Nepal earthquake decreases substantially showing a similar trend as that of the pattern obtained by Sharma et al. (2009). Although the generalised trend is following the relation of Sharma et al. (2009) but some of the stations exhibits PGA contrary to this relation which happens due to the rupture directivity. In order to see the difference of PGA decay in SW and SE direction of the mainshock we have plotted the PGA versus distance for both the directions as shown in Fig. 5b. It is observed that the decay pattern although is the same in both the directions but the PGA values are relatively higher in the SE direction of the mainshock as compared with the PGA values in the SW direction to the mainshock and this may be explained due to the rupture directivity of the mainshock mainly in the SE of the mainshock location. In this study, we attempted to show the attenuation relation with distance by simply plotting the variation of the estimated PGA with the hypocentral distance, which helps in understanding the trend of the variation (Fig. 5a). The estimates of PGA are not derived from the relationship of Sharma et al. (2009), rather the actual variation of the PGA for the recorded accelerograms and its correspondence to the structural heterogeneities are interpreted. Thus, at few sites the distance and PGA relationship varies, this happens because of the rupture directivity. Our estimates of PGA, PGV and PGD values are shown in Tables 2a and 2b for the mainshock and its other strong aftershocks. Fig. 6

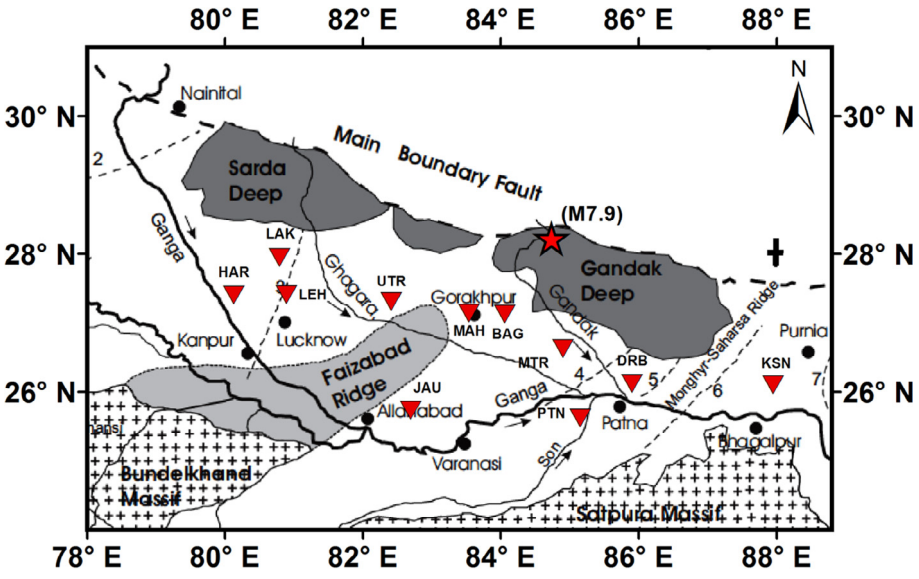

Fig. 3. Subsurface geology and tectonic framework of the upper & middle Ganga basin. Also Sarda Deep & Gandak Deep and Faizabad ridge & Monghyr Saharsa Ridge are shown here. 1 - Great Boundary Fault, 2 - Delhi-Moradabad Fault, 3 - Lucknow Fault, 4 - west Patna Fault, 5 - East Patna Fault, 6 - Monghyr-Saharasa Ridge Fault, 7 - Malda-Kishanganj Fault (modified after Sinha et al., 2005).

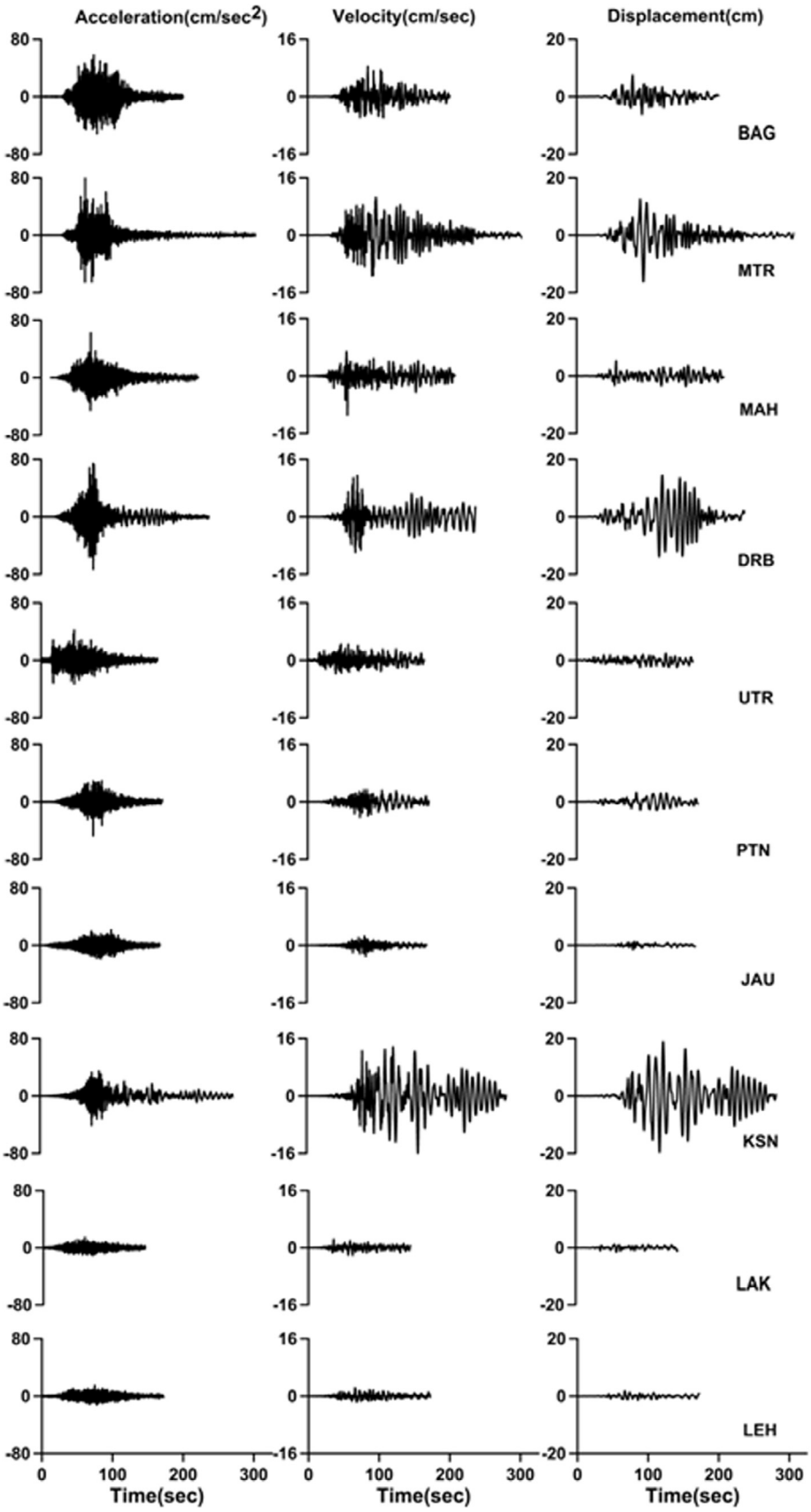

Fig. 4. Plots of PGA (acceleration in cm/sec^2), PGV (velocity in cm/sec) & PGD (displacement in cm) estimated for the main-shock of 25th April 2015 (Mw 7.9) at the sites in eastern UP and northern Bihar states of India bordering Nepal.

Table 2a
PGA, PGV and PGD values observed for Nepal earthquake of 25th April 2015 (Mw 7.9).

Date	Time (IST) (hh:mm)	Station	Magnitude (Mw)	PGA (cm/sec^2)	PGV (cm/sec)	PGD (cm)	Distance from event (kms)
25/04/2015	11:41	BAG	7.9	58	8	7	120
25/04/2015	11:41	MAH	7.9	63	11	5	149
25/04/2015	11:41	MTR	7.9	80	11	16	166
25/04/2015	11:41	DRB	7.9	74	12	14	210
25/04/2015	11:41	UTR	7.9	42	5	3	233
25/04/2015	11:41	PTN	7.9	47	4	3	281
25/04/2015	11:41	JAU	7.9	22	3	1	325
25/04/2015	11:41	LAK	7.9	15	2	2	358
25/04/2015	11:41	LEH	7.9	14	2	2	373
25/04/2015	11:41	KSN	7.9	41	16	20	399
25/04/2015	11:41	HAR	7.9	9	2	2	447

Table 2b
PGA values observed in case of strong aftershocks related to Nepal earthquake.

Date	Time (IST) (hh:mm)	Station	Magnitude (Mw)	PGA (cm/sec^2)	Distance from event (kms)
25/04/2015	12:15	BAG	6.6	23	130
25/04/2015	12:15	MAH	6.6	12	164
25/04/2015	12:15	MTR	6.6	38	164
25/04/2015	12:15	UTR	6.6	28	251
25/04/2015	12:15	PTN	6.6	12	278
25/04/2015	12:15	KSN	6.6	9	383
25/04/2015	12:15	LEH	6.6	8	392
26/04/2015	12:39	MTR	6.9	47	146
26/04/2015	12:39	BAG	6.9	36	189
26/04/2015	12:39	KUS	6.9	34	232
26/04/2015	12:39	KSN	6.9	20	263
26/04/2015	12:39	TUL	6.9	22	345
26/04/2015	12:39	UTR	6.9	15	348
26/04/2015	12:39	JAU	6.9	11	381
26/04/2015	12:39	LEH	6.9	7	495
12/05/2015	12:35	MTR	7.3	69	161
12/05/2015	12:35	KSN	7.3	28	263
12/05/2015	13:06	KSN	6.2	9	248
26/04/2015	12:39	MAH	6.9	23	239

represents the distribution of PGA, PGV and PGD during the earthquake shaking of the mainshock, which clearly demonstrates a distinct partitioning in the estimates of higher and lower values with respect to the mainshock orienting in the SE and SW direction, respectively. The principal cause of partitioning may be due to several causes, such as varied earthquake radiation pattern, stiffness of the sub-surface formations, and the geo-morphological barriers that may have retarded or accelerated the seismic wave propagation differently with the lapse of time in SE and SW direction (Fig. 6).

3.1. Variation of PGD, PGV and PGA

Based on the distance of SMA sites from the mainshock, initially it was observed that attenuation of seismic wave and changes in PGA & PGV values are very much related to the geometrical spreading with respect to the mainshock. It is evident from the distribution of SMA stations (Fig. 2) that the site BAG located at 120 km showed PGA estimate of 58 cm/sec^2 (PGV of 8 cm/sec), while HAR located at the epicentre distance of 447 km with estimate of PGA of 9 cm/sec^2 (PGV of 2 cm/sec) (Fig. 6; Tables 2a and 2b). Such correlation of estimated values of PGA and PGV with epicentre distance is found valid for most of the stations. Contrary to this, the analyses of estimated values of PGA and PGV made for other SMA stations (e.g., BAG, MTR) showed negative correlation and were not strictly abide by the law of geometrical spreading that governs the extent of seismic wave attenuation. As described above, SMA stations, MTR located at the epicentre distance of 166 km and showed the highest values of PGA as 80 cm/sec^2 with PGV of 11 cm/sec. The SMA station of KSN located at the distance of 399 km from the mainshock, which showed PGA of 41 cm/sec with PGV of 16 cm/sec (Table 2a). It is spectacular to note that values of PGA, PGV and PGD estimated for SMA stations (e.g., MAH, UTR, LEH) located in the eastern UP state of India showed decreasing trend beyond the Faizabad ridge downwardly to the SW direction of the mainshock, while the increasing pattern of PGV and PGD is observed at SMA stations located in the Bihar State of India (e.g., BAG, MTR, KSN) beyond the Monghyr-Saharsa Ridge downwardly to the SE direction of the mainshock, which is the rupture direction of the mainshock (Figs. 3 and 6). Similarly, it is found that there is no systematic correspondence in variation of the estimated values of PGA and PGV with epicentre distance for SMA stations (e.g., BAG, MTR, HAR, KSN) located in the eastern Uttar Pradesh (Fig. 6 and Tables 2a and 2b), which suggests that sub-surface material heterogeneities and geo-mechanical strength of the seismic propagating media are the principal factors that might have controlled the variation in PGA, PGV, and PGD estimates due to prevalence of intrinsic attenuation of sub-surface layers, that have strong bearing on geological vulnerability that controlled the degree of damage to structures. It is observed that the rupture directivity plays an important role in varying estimates of PGA, PGV and PGD for stations located in the SE and SW to the mainshock

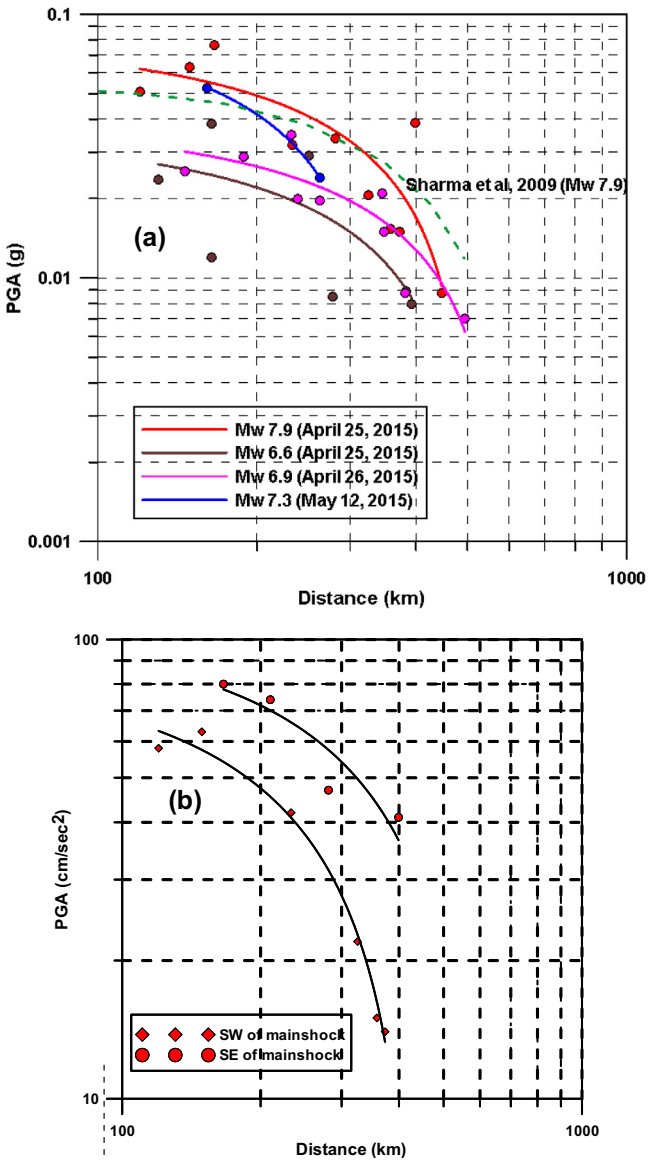

Fig. 5. (a) Observed PGA distribution with respect to distance from main-shock and associated strong earthquakes with all available SMA data for Uttar Pradesh and Bihar stations. PGA for main-shock of Mw 7.9 is compared with attenuation relationship estimated by Sharma et al. (2009) for Himalayan region. (b) Distribution of PGA in SE and SW direction of the main-shock rupture.

beneath the study area (Figs. 2 and 6). The rupture directivity suggests that the propagation of the mainshock rupture dominantly in a particular direction (SE) to the mainshock of the 2015 Nepal Earthquake (Mw 7.9).

3.2. Geo-morphological constraints and rupture propagation

Geo-morphological constraints play an important role in controlling the extent of earthquake rupture propagation. The existence of Faizabad Ridge (FR) in the SW direction to the downward of the Mainshock might have hindered the rupture propagation of the mainshock towards SW, while the rapid and uninterrupted propagation of the mainshock rupture towards SE to that of the mainshock justifies the concentration of almost all aftershocks in the SE direction of the mainshock ruptured zone (Fig. 1). It is, however, to be mentioned that the increasing estimates of PGA values showed no correlation in the prominent rupture direction towards SE. The lower value of PGA of 41 cm/sec^2 at KSN beyond the Monghyr Saharsa Ridge (MSR) suggests that the ridge might have retarded the seismic wave acceleration generated by the mainshock. Consequently, despite the possibly similar sub-surface formational conditions towards the SE it was the geo-morphological barriers that might have played a role in reducing the PGA values farthest to SE and SW of the mainshock rupture. In order to ascertain the role of sub-surface formational and compositional scenario, we critically analyzed the variation trend of PGD and PGV as shown in Fig. 6 with estimates of values in Table 2a. It is intriguing to see that the values of PGA started to decrease further to SE direction beyond the MSR that suggests that this Ridge might have acted as a barrier to retard the mainshock rupture propagation beyond the longitude of 87.5 degree east (Fig. 6). These observations are in good agreement with the lower estimates of PGA made for beyond the FR in the SW direction and beyond the MSR in the SE direction, while higher values of these parameters in the SE direction supports the idea that the sub-surface media for seismic wave propagation is a key factor to control the nature and extent of the PGA, PGV and PGD. It is observed that ridge associated with thicker and compact meta-sedimentary formation has tendency to retard the seismic wave propagation through the attenuation and dispersion of seismic wave (Pollitz and Mooney, 2015). Recent study showed that the character of the regional seismic-wave propagation gets affected by the passage of seismic wave through the contrasting terrains associated with the intricate geo-morphological structures (Pollitz and Mooney, 2015). Higher estimates of PGD and PGV at the station, KSN towards the SE of the mainshock rupture beyond the MSR suggests that the zone beyond the ridge may be associated with comparatively crystalline and compact rock materials with relatively less deformed and greater stiffness coefficient of the sub-surface layers. The hindrance of seismic wave is not related to the causative fault as causative faults are the generator of the seismic waves radiated in different directions. The nature and extent of the radiated seismic wave be dictated by the structural heterogeneities, geomorphological and geomorphotectonic structures associated with the source region. The seismic wave amplitude may be enhanced, retarded or terminated depending on the strength and type of geomorphotectonic structures. In this study, we found that the amplitude of the seismic waves might have modified due to presence of FR and MSR. This interpretation is found in unison to the geomorphological study of the area made by Sinha et al. (2005). They described that the Indo-Gangetic plain was associated with major and active faults with localized deformational changes, which may have caused sufficient influence on the geomorphology of the study area, where the recent Nepal earthquake shook the Indo-Gangetic plain with different degree of shaking.

Sometimes, the site conditions may be the cause of the amplification or de-amplification of the ground acceleration. The Peak Ground Velocity (PGV) varies from 1 to 16 cm/sec while the Peak Ground Displacement (PGD) lies in between 1 cm and 20 cm for the same sites. As mentioned above, Table 2a presents the combined values of PGA, PGV and PGD estimated from the Main earthquake of 25th April 2015 at the sites located in the eastern UP and northern Bihar. The thickness of the alluvium is reported of about 6 km near the foothill zone of Gangetic plain and it decreases gradually towards south (Rao, 1973). This report is also supported by the geophysical surveys conducted in the area that clearly exhibits the presence of metamorphic basement with some ridges and basins in the Gangetic plain area (Fig. 3). Based on the density Moho relief and rheological study using comprehensive gravity estimates along the Indo-Gangetic plains, thinning of the crust around 35–36 was also reported for the area (Mishra et al., 2004), which may be due to flexure of the Indian plate caused by the load of the Himalayas.

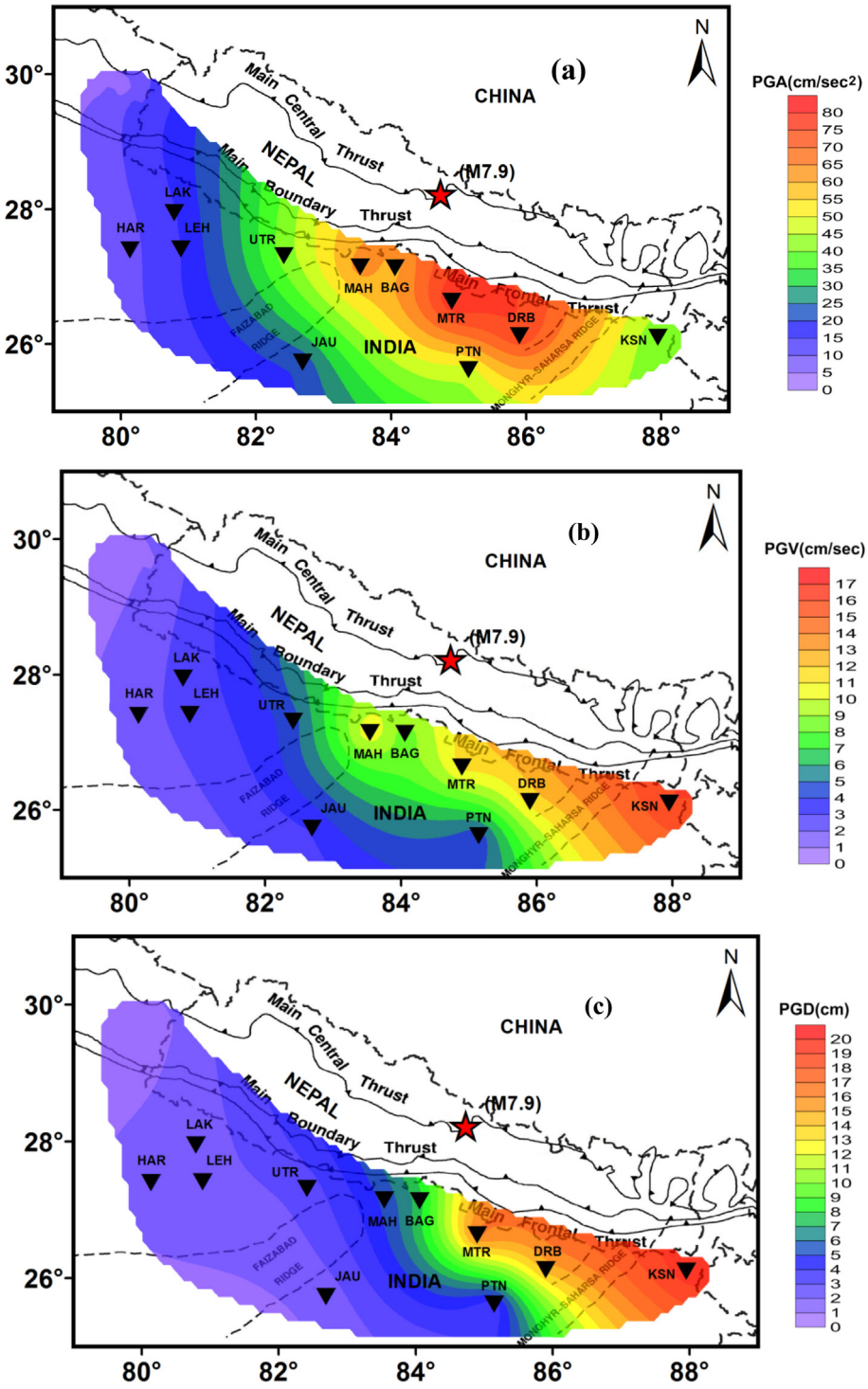

Fig. 6. Observed PGA (a) and calculated PGV (b) & PGD (c) distribution during the main-shock of 25th April 2015 (Mw 7.9) for the sites in UP and Bihar.

The extent of damage due to great to major earthquakes is dictated by the size and impacts of the generating earthquake, which in turn related to the compactness of geo-morphological and the embedded structural heterogeneities of the source zone where the process of strain accumulation continues to bring the brittle failure. This geological condition makes the study region highly vulnerable in case of earthquake hazards especially in the central seismic gap. There is a serious debate on the issue that whether the Nepal earthquake occurred in the central seismic gap zone what was expected as the asperity for generating the great to major earthquakes (Bilham and Wallace, 2005). The Nepal earthquake may not be a gap filling earthquake because it is not a great earthquake while the central seismic gap region has the potential to generate a great earthquake (Gupta and Gahlaut, 2014, 2015). The recent review by Mishra (2014a,b) argued that the seismic gap zone is the zone where big/great earthquake so far not occurred with emphasis that all gap zones cannot be regarded as the zones of impending big earthquake in future. It is so because types of structural heterogeneities (weak and strong) control the strength of generating earthquakes beneath the seismic gap zones (Wang et al., 2006; Mishra, 2014a,b). Moreover, the extent of damage is related to the amplification of the

sub-surface foundational formations beneath the structure during shaking of the earthquake. The presence of the lesser Himalayan sedimentary rocks cause significant bearing on the degree of damage to the structures (Shanker et al., 2011). It is pertinent to note that our most of SMA stations are located in the Indo-Gangetic plains having neo-gene Quaternary sediments, which are plausibly apt to the genesis of low velocity beneath the sub-surface layers (Rao, 1973; Shanker et al., 2011).

3.3. Strong motion and extent of damage

We analyzed the strong motion waveform data recorded by station located at Kishanganj (KSN) with the condition to estimate the excitation of the pulse for the lesser thickness of the sediments beneath KSN in comparison to that of Indo-Gangetic sites where most of our SMA stations are located. Our analysis showed that the excitation pulse became dominant for the estimate of peak horizontal ground velocity of 20 cm/sec. The net effect of long duration waveform produced at KSN gets resonated in the medium. Also the rupture directivity in the SE direction from the mainshock towards KSN might have played an important role for greater values of PGV and PGD at KSN. The intensity at KSN was reported V (USGS, 2015) with no considerable damage reported in the district town of Kishanganj of Bihar, which may be because of lesser peak ground acceleration (PGA = 41 cm/sec^2) in comparison to those values estimated for other SMA stations located at Darbhanga (DRB) [PGA = 73 cm/sec^2] and Motihari (MTR) [80 cm/sec^2], another district towns of Bihar. Appreciable damages to structures along with death of about 52 people were reported in India out of which 25 were from Bihar and 24 from UP, during the mainshock according to the media report by Hindustan Times on 25th April 2015. Motihari (MTR) and Darbhanga (DRB) district towns showed intensity of VI on MMI scale during Nepal Earthquake and it is important to mention that there were huge damages to structures and the death of people occurred in these two cities (Darbhanga and Motihari), bordering Nepal during the past 1934 Bihar – Nepal earthquake (M 8.2) and the 1988 Darbhanga earthquake (Mw 6.8), which in turn suggests that there is either to implement the older Building Design Codes strictly or to develop suitable Building design codes for strict implementations to mitigate the earthquake risks and hazards of cities of Indian states bordering Nepal.

4. Response spectra of Nepal earthquake and its relevance to BIS 2002 code

Normalised response spectra are determined at 5% damping from the strong ground motions recorded by several SMAs deployed in Indian states of UP and Bihar (Figs. 2 and 3). Fig. 7a shows the response spectra for horizontal components recorded in UP and Bihar sites. It is observed that stations located over alluvium deposits show a peak of average response at 0.242 sec for horizontal component, while the average response spectra for the vertical component showed maximum amplification at the period of 0.193 sec (Fig. 7b). The horizontal component detects the particle motion in perpendicular to the direction of motion due to which, the response spectra gets delayed to obtain the higher periods. On the other hand the vertical component detects the particle motion in the direction of propagation of the wave which results the spectra peak to be obtained at low period than the horizontal component. It has been observed that our acceleration response spectra at all sites are of similar type of shape due to Indo-Gangetic Neogene Quaternary sediments, indicating that the acceleration response spectra get influenced by the local site conditions. Our designed response spectra found to depict dominating amplification for the horizontal components at maximum period than those of vertical components, which are unison to the standard norms.

Raghukanth and Iyengar (2007) showed that the response spectrum in Indian code (BIS, 2002) underestimates seismic forces at high frequency for rock sites; while at soft soil sites it overestimates forces at low frequencies. Chopra and Choudhury (2011) argued that for a period greater than 0.4 sec the spectral amplifications are overestimated in Indian code both for soft soil and rock sites; while, for periods below 0.1 sec, the spectral accelerations are underestimated. Studies made by other researchers suggested that different site conditions can induce amplifications at different periods in the response spectra (Seed et al., 1976; Mohraz, 1976), which are derived from the estimate of spectral acceleration for different geological formations in diverse tectonic conditions elsewhere in the world (Mandal et al., 2013; Chowdhuri et al., 2008). Some of the researchers suggested that the nonlinearity affects ground motions from a major/great earthquake significantly because of their close correspondence with material heterogeneities of the seismic wave propagating media beneath the study region (Su et al., 2006; Raghukanth and Iyengar, 2007; Chopra and Choudhury, 2011). At large distances, the average soil site shows higher amplitudes in spectra at all frequencies than that of rock sites, but at short distances, in the presence of nonlinearity, the high frequency part of the spectra shows smaller amplitudes on soil sites than that on rock sites. In the present study, the nonlinearity plays an important role in case of Nepal earthquake for normalised Spectral Amplification (SA) as shown in Fig. 7a-(i)–a-(iv) for stations BAG, MTR, DRB and KSN respectively. The response spectra of KSN show additional peaks at later periods as shown in Fig 7a-(iv). This may be the reason for the pulse excitation and resonance effects experienced by this site in order to get higher PGV and PGD. Similar effect is also obtained by MTR and DRB sites which showed more damage during Nepal earthquake. Generally, the normalised SA values are not much important; the main important point here is the dominant period. If we carefully see the Normalised SA for individual stations at the farthest distances the Normalised SA becomes complicated and at far stations we get the peaks at the later periods which are more at in the direction of rupture of the mainshock. BAG being the nearest station shows a single peak while at MTR being the southern station shows various peaks, which suggest that the duration of the wave propagation is more at MTR than BAG. Similarly, DRB being in SE direction shows more SA and KSN being the farthest station shows more SA and also generates peaks at later periods in order to satisfy the pulse excitation and resonance effects (Galetzka et al., 2015). Fig. 7c shows the site amplification using the SMA data recorded at four sites (i.e. BAG, DRB, MTR and KSN). This amplification corresponds to the horizontal to vertical ratio in order to see the amplification of these particular sites. However, it is observed that the site BAG had relatively more amplification in comparison to other three sites. It may suggest softness of the material beneath BAG than that of DRB, MTR and KSN. It is also confirmed by Sinha et al. (2005) that in Indo-Gangetic plain the sedimentary thickness decreases as we go towards the south. MTR shows least amplified while the DRB and KSN show amplified peak at 2.3 Hz (two peaks) and 7.1 Hz respectively. Again DRB shows one more peak at 5.1 Hz which indicates the association of damage incurred here in case of Nepal Earthquake due to site amplification as one of the factor. It is worthwhile to mention that BAG site is more influenced by the site effect than MTR. The site of MTR found to be associated with maximum PGA, which is a function of source, path and site. The site of MTR falls in SE direction from the mainshock which is influenced by rupture directivity and also showed considerable damage due to the maximum PGA obtained amongst all the sites in the study region. Similarly DRB and KSN are amplified with a considerable amount of PGA. Thus we can infer that the site amplification

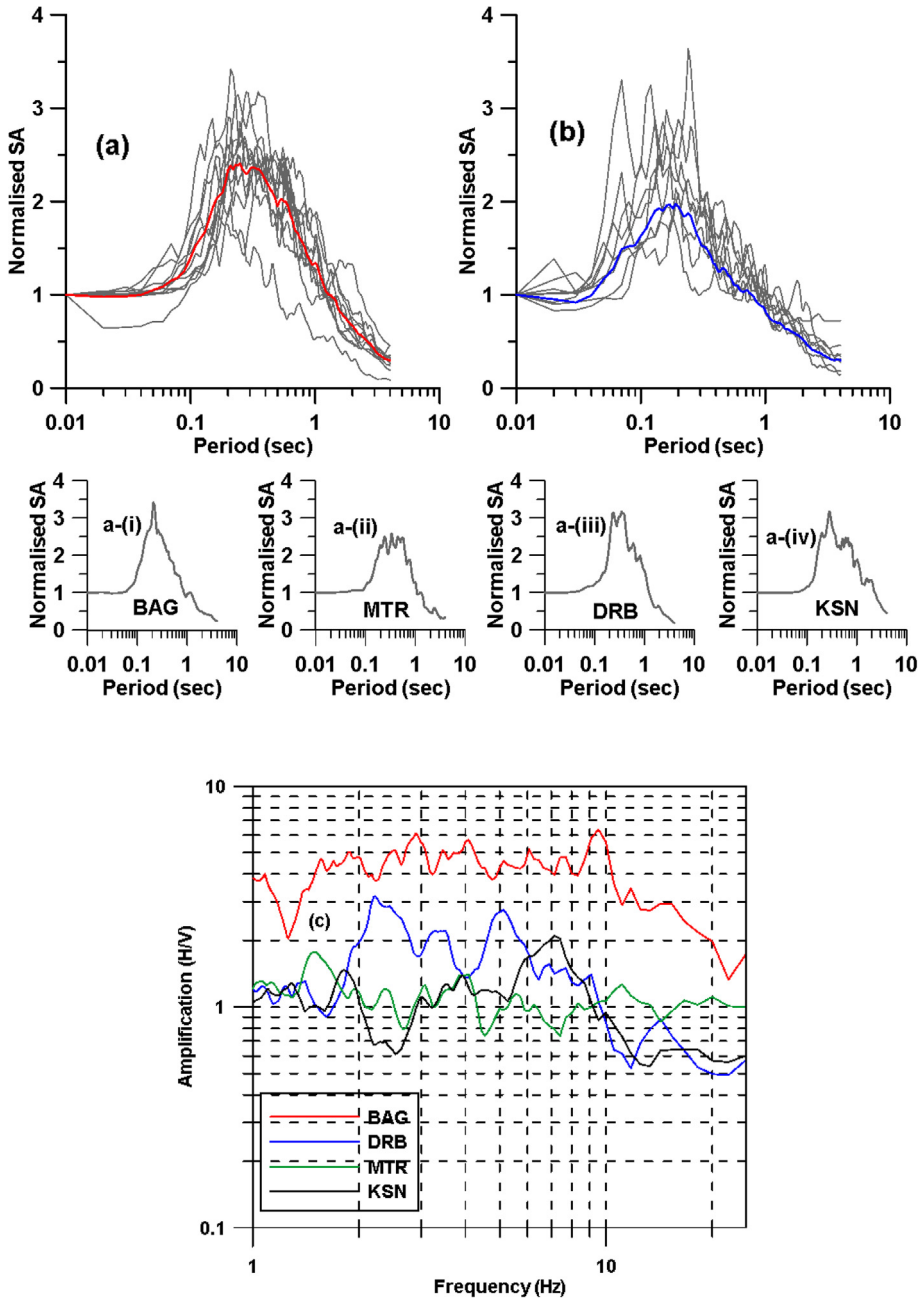

Fig. 7. Normalised SA at sites on Alluvium (Quaternary) for average of horizontal components (red line) (a), vertical components (blue line) (b) and grey colour lines are the normalised SA of various stations. BAG, MTR, DRB and KSN stations normalised SA are presented in a-(i), a-(ii), a-(iii) and a-(iv) respectively. (c) Estimated H/V with respect to the frequency for BAG, DRB, MTR and KSN. (For interpretation of the references to colour in this figure legend, the reader is referred to the web version of this article.)

has strong bearing on the shallow sub-surface sediments, while PGA takes care of the entire sub-surface strata containing bedrock and shallow sub-surface sediments.

The response spectra assimilated in this study using the records from horizontal and vertical components by SMA stations (Fig. 7a and b). The average response spectra of both horizontal components are compared with the Bureau of Indian Standard (BIS, 2002) codes, which are applicable for the seismic forces and are used in construction engineering practices in India (Fig. 8). It is found that our average response spectra assimilated for horizontal component are found to fall within the limit of the average response spectra generated by BIS-2002 with a similar pattern of variation for our study area associated with alluvial Indo-Gangetic Neogene sediments (Fig. 8). The damage occurred at few sites of UP and Bihar was due to the poor construction practices used by the people. The present damage scenario that occurred aftermath of the 25th April 2015 Nepal earthquake (Mw 7.9) in the northern Bihar and eastern UP of India bordering Nepal demonstrates that the existing BIS-2002 code has not been applied in constructing structures and buildings in the areas that showed maximum damage during earthquake shaking. In order to minimize the degree of damage and loss of lives in the border areas of India to Nepal, it is imperative to implement the existing BIS-2002 codes under earthquake risk mitigation strategy by developing earthquake risk resilient buildings and structures. Also it is important to be noted that the building design code based on several constraints of geo-mechanical properties of sub-surface materials derived from seismic microzonation may have strong deportment to minimize the huge loss of life and property during future damaging hazardous earthquakes in Himalaya (Mishra, 2012).

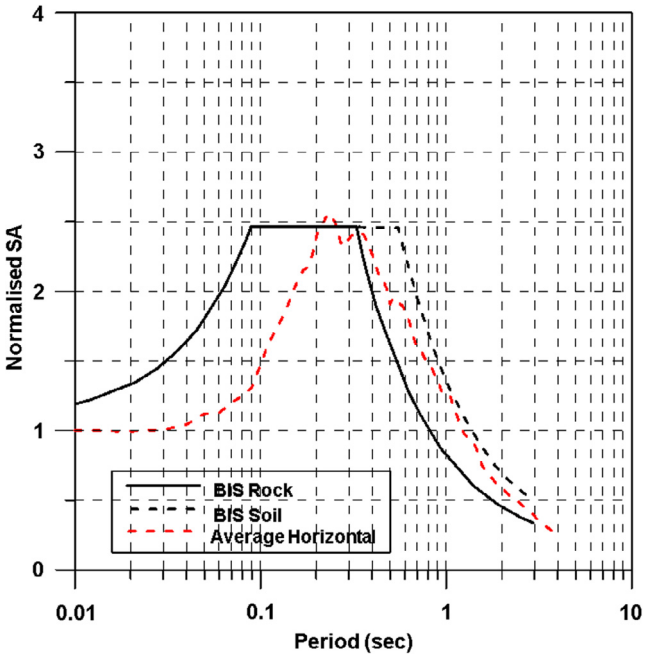

Fig. 8. Comparison of average response spectrum for the main earthquake of 25th April 2015 (Mw 7.9) with BIS-2002 code.

5. Conclusions

The Nepal earthquake (Mw 7.9) occurred on 25th April 2015 with a subsequent major earthquake (Mw 7.3) on 12th May 2015 in the Central seismic gap region of Himalaya which is extending from the 1905 Kangra earthquake to the 1934 Bihar-Nepal earthquake. Our estimates of PGA, PGV and PGD values using SMA data of Nepal Earthquake are found varied with varying pattern in both SE and SW of the Mainshock around the Indo-Gangetic plain comprising eastern UP and northern Bihar. The pattern represents the distribution of PGA, PGV and PGD during the earthquake shaking of the mainshock, which clearly demonstrates a distinct partitioning in the estimates of higher and lower values with respect to the mainshock orienting in the SE and SW direction, respectively. The principal cause of partitioning may be due to several causes, such as varied earthquake radiation pattern, the stiffness of the subsurface formations, and the geo-morphological barriers that may have retarded or accelerated the seismic wave propagation differently with the lapse of time in SE and SW direction. Geomorphological constraints play an important role in controlling the extent of earthquake rupture propagation. The existence of Faizabad Ridge located downward to the Mainshock might have hindered the propagation of seismic waves generated by the mainshock towards SW, while the rapid and uninterrupted propagation of the seismic waves towards SE to the mainshock justifies the concentration of almost all aftershocks in the SE direction of the mainshock ruptured zone. Estimated normalised response spectra found to depict dominating amplification for the horizontal components at maximum period than those of vertical components, which are unison to the standard norms of the SMA estimates. In order to minimize the degree of damage and loss of lives in the border areas of India and Nepal, it is imperative to implement the existing BIS-2002 codes under earthquake risk mitigation strategy by developing earthquake-resilient buildings and structures. Thus, we can conclude that, the existing BIS-2002 code may be applicable for Himalayan Border states as our response curves estimated at all periods for alluvial sites using SMA data of Nepal mainshock and its associated strong shocks fall within the structural limits proposed by BIS-2002 code (Fig. 8). We can infer that the structural designs if followed based on BIS-2002 in northern Bihar and Eastern Uttar Pradesh could have sustain the earthquake shaking during the 2015 Nepal mainshock and its strong aftershocks. It is, therefore we can suggest that implementation of the suitable building design code based on several constraints of geomechanical properties of sub-surface materials derived from seismic microzonation may have strong bearing on minimizing the loss of lives and property during future damaging earthquakes in Himalaya.

Acknowledgements

Authors sincerely thank Dr. Shailesh Nayak, Former Secretary, Ministry of Earth Sciences and Distinguished Professor and Scientist, Ministry of Earth Sciences, for his consistent motivation and lesson on the interpretation of the results of SMA data. Dr. V.K. Gahlaut, Director, National Centre of Seismology (NCS), and entire team of NCS (Dr. G. Suresh, Mr. P.R. Baidya, Mr. H.P. Shukla; Mr. J.L. Gautam; and Mr. R.K. Singh) are gratefully acknowledged for stimulating discussion and encouragement to accomplish this piece of research. Authors are also thankful to Prof. Ashok Kumar, IIT Roorkee and his team for managing the SMA stations in different parts of Himalayan region. We also acknowledge Dr. Sanjay Prajapati, Scientist, NCS for data acquisition from field.

References

Aki, K., Chouet, B., 1975. Origin of the coda waves: source attenuation and scattering effects. J. Geophys. Res. 80, 3322–3342.

Avouac, J.F., Meng, L., Wei, S., Wang, T., Ampuero, J.P., 2015. Lower edge of locked Main Himalayan Thrust unzipped by the 2015 Gorkha earthquake. Nat. Geosci. ISSN 1752-0894.

Bilham, R., Wallace, K., 2005. Future *Mw* > 8 earthquakes in the Himalaya: implications from the 26 December 2004 *Mw* = 9.0 earthquake on India's eastern plate margin. Geol. Surv. India Spec. Publ. 85, 1–14.

Bilham, R., 2015. Raising Kathmandu. Nat. Geosci. 8, 582–584.

BIS, 2002. Criteria for earthquake resistant design of structures, part I—general provisions and buildings. Bureau of Indian Standards. IS 1893 [part I].

Cattin, R., Avouac, J.P., 2000. Modeling mountain building and the seismic cycle in the Himalaya of Nepal. J. Geophys. Res. 105, 13389–13407. http://dx.doi.org/10.1029/2000JB900032.

Center for Disaster Management and Risk Reduction Technology (CEDIM), 2015. Nepal Earthquakes – Report #3 Available at: <https://www.cedim.de/english/index.php>.

Chopra, S., Choudhury, P., 2011. A study of response spectra for different geological conditions in Gujarat, India. Soil Dynam. Earthq. Eng. 31, 1551–1564.

Chowdhuri, S.N., Singh, O.P., Mishra, O.P., Kayal, J.R., 2008. Microzonation study from ambient noise measurement for assessing site effects in Krishnagar area and its significance with the damage pattern of Ms 4.3 of the 24th September, 1996 earthquake. Spec. Iss. Indian Miner. 61 (3–4), 183–192.

DeCelles, P.G., Robinson, D.M., Quade, J., Ojha, T.P., Garzione, C.N., Copeland, P., Upreti, B.N., 2001. Stratigraphy, structure, and tectonic evolution of the Himalayan fold-thrust belt in western Nepal. Tectonics 20 (4), 487–509.

Denolle, M.A., Fan, W., Shearer, P.M., 2015. Dynamics of the 2015 *M*7.8 Nepal earthquake. Geophys. Res. Lett. 42 (18), 7467–7475. http://dx.doi.org/10.1002/2015GL065336.

Fan, W., Shearer, P.M., 2015. Detailed rupture imaging of the 25 April 2015 Nepal earthquake using teleseismic P waves. Geophys. Res. Lett. 42, 5744–5752. http://dx.doi.org/10.1002/2015GL064587.

Feng, G., Li, Z., Shan, X., Zhang, L., Zhang, G., Zhu, J., 2015. Geodetic model of the 2015 April 25 *Mw* 7.8 Gorkha Nepal Earthquake and *Mw* 7.3 aftershock estimated from InSAR and GPS data. Geophys. J. Int. 203, 896–900. http://dx.doi.org/10.1093/gji/ggv335.

Gansser, A., 1964. Geology of the Himalayas. Wiley-Interscience, New York.

Galetzka, J., Avouac, J.F., Genrich, J.F., Hudnut, K.W., 2015. Slip pulse and resonance of the Kathmandu basin during the 2015 Gorkha earthquake, Nepal imaged with geodesy. Science, ISSN 0036-8075.

Gupta, H.K., Gahlaut, V.K., 2014. Seismotectonics and large earthquake generation in the Himalayan region. Gondwana Res. 25, 204–213.

Gupta, H.K., Gahlaut, V.K., 2015. Can an earthquake of Mw ~ 9 occur in the Himalayan region. The Geological Society London, Special Publication no. 412. http://dx.doi.org/10.1144/SP412.10.

Herman, F., Copeland, P., Avouac, J.P., Bollinger, L., Maheo, G., Le Fort, P., Rai, S., Foster, D., Pecher, A., Stuwe, K., Henry, P., 2010. Exhumation, crustal deformation, and thermal structure of the Nepal Himalaya derived from the

inversion of thermochronological and thermobarometric data and modeling of the topography. J. Geophys. Res. 115, B06407. http://dx.doi.org/10.1029/2008JB006126.
Khattri, K.N., Tyagi, A.R., 1983. Seismicity patterns in the himalayan plate boundary and identification of the areas of high seismic potential. Tectonophysics 96, 281–297.
Khattri, K.N., 1987. Great earthquakes, seismicity gaps and potential to earthquake disaster along the Himalayan plate boundary. Tectonophysics 138, 92–99.
Khattri, K.N., 1999. An evaluation of earthquake hazard and risk in northern India. Himalayan Geol. 20, 1–46.
Kumar, A., Mittal, H., Sachdeva, R., Kumar, A., 2012. Indian national strong motion network. Seismol. Res. Lett. 83 (1), 29–36.
Lindsey, E., Natsuaki, R., Xu, X., Shimada, M., Hashimoto, H., Melgar, D., Sandwell, D., 2015. Line of sight deformation from ALOS-2 interferometry: Mw 7.8 Gorkha Earthquake and Mw 7.3 aftershock. Geophys. Res. Lett. 42, 6655–6661. http://dx.doi.org/10.1002/2015GL065385.
Mandal, H.S., Shukla, A.K., Khan, P.K., Mishra, O.P., 2013. A new insight into probabilistic seismic hazard analysis for Central India. Pure Appl. Geophys. 170 (12), 2139–2161.
Mishra, D.C., Laxman, G., Arora, K., 2004. Large wavelength gravity anomalies over the Indian continent: indicators of lithospheric flexure and uplift and subsidence of Indian Peninsular Shield related to isostasy. Curr. Sci. 86, 861–867.
Mishra, O.P., 2012. Applications of information technology in Disaster Risk Management with reference to South Asia Disaster Knowledge Network (SADKN) and Digital Vulnerability Atlas of South Asia. In: *5th Asian Ministerial Conference on Disaster Risk Reduction (5th AMCDRR)*, 22–25 October 2012 at Yogyakarta, Indonesia.
Mishra, O.P., 2014a. Intricacies of the Himalayan seismotectonics and seismogenesis: need for integrated research. Curr. Sci. 106 (2), 176–187.
Mishra, O.P., 2014b. Seismological research in India (2007–2011). Proceeds Indian National Science Academy (PINSA) 76 (3), 361–375.
Mitra, S., Himangshu, P., Ajay, K., Shashwat, K.S., Siddharth, D., Debarchan, P., 2015. The 25 April 2015 Nepal earthquake and its aftershocks. Curr. Sci. 108 (10), 1938–1943.
Mittal, H., Gupta, S., Srivastava, A., Dubey, R.N., Kumar, A., 2006. National strong motion instrumentation project: an overview. In: 13th Symposium on Earthquake Engineering, Indian Institute of Technology, Roorkee, Dec 18–20. Elite Publishing, New Delhi, pp. 107–115.
Mohraz, B., 1976. A study of earthquake response spectra for different geological conditions. Bull. Seismol. Soc. Am. 66 (3), 915–935.
Nakata, T., 1989. Active faults of the Himalayas of India and Nepal. Spec. Pap. Geol. Soc. Am. 232, 243–264.
Ni, J., Barazangi, M., 1984. Seismotectonics of the Himalayan collision zone: geometry of the underthrusting Indian plate beneath the Himalaya. J. Geophys. Res. 89, 1147–1163.
Pandey, M.R., Tandukar, R.P., Avouac, J.P., Lave, J., Massot, J.P., 1995. Interseismic strain accumulation on the Himalayan crustal ramp (Nepal). Geophys. Res. Lett. 22, 751–754.
Pandey, M.R., Tandukar, R.P., Avouac, J.P., Vergne, J., Héritier, T., 1999. Seismotectonics of Nepal Himalayas from a local seismic network. J. Asian Earth Sci. 17, 703–712. http://dx.doi.org/10.1016/S1367-9120(99)00034-6.
Parameswaran, R.M., Natarajan, T., Rajendran, K., Rajendran, C.P., Mallick, R., Wood, M., Lekhak, H.C., 2015. Seismotectonics of the April–May 2015 Nepal earthquakes: an assessment based on the aftershock patterns, surface effects and deformational characteristics. J. Asian Earth Sci. 111, 161–174.
Pollitz, F.F., Mooney, W.D., 2015. Regional seismic-wave propagation from the M5.8 23 August 2011, Mineral, Virginia, earthquake. Geol. Soc. Am. Spec. Pap. 509, 95–116. http://dx.doi.org/10.1130/2015.2509 (06).
Raghukanth, S.T.G., Iyengar, R.N., 2007. Estimation of seismic spectral acceleration in Peninsular India. J. Asian Earth Sci. 116, 199–214.
Rajendran, C.P., John, B., Rajendran, K., 2015. Medieval pulse of great earthquakes in the central Himalaya: viewing past activities on the frontal thrust. J. Geophys. Res. 120, 1623–1641. http://dx.doi.org/10.1002/2014JB011015.
Rao, M.B.R., 1973. The subsurface geology of the Indo-Gangetic plains. J. Geol. Soc. India 14, 217–242.
Robert, X., van der Beek, P., Braun, J., Perry, C., Mugnier, J.L., 2011. Control of detachment geometry on lateral variations in exhumation rates in the Himalaya: insights from low-temperature thermochronology and numerical modeling. J. Geophys. Res. 116, B05202. http://dx.doi.org/10.1029/2010JB007893.
Robinson, D.M., DeCelles, P.G., Garzione, C.N., Pearson, O.N., Harrison, T.M., Catlos, E. J., 2003. Kinematic model of the Main Central Thrust in Nepal. Geology 31 (4), 359–362.
Schelling, D., Arita, K., 1991. Thrust tectonics, crustal shortening and the structure of the Far Eastern Nepal Himalaya. Tectonics 10, 851–862.
Seeber, L., Armbruster, J.G., Quittmeyer, R.C., 1981. Seismicity and continental subduction in the Himalayan arc. Am. Geophys. Union, Geodynam. Ser. 3, 215–242.
Seed, H.B., Ugas, C., Lysmer, J., 1976. Site dependent spectra for earthquake-resistant design. Bull. Seismol. Soc. Am. 66, 221–243.
Shanker, D., Paudyal, H., Singh, H.N., 2011. Discourse on seismotectonics of Nepal Himalaya and vicinity: appraisal to earthquake. Geosciences 1 (1), 1–15. http://dx.doi.org/10.5923/j.geo.20110101.01.
Sharma, M.L., Douglas, J., Bungum, H., Kotadia, J., 2009. Ground-motion prediction equations based on data from the Himalayan and Zagros Regions. J. Earthquake Eng. 13, 1191–1210.
Sharma, B., Chopra, S., Sutar, A.K., Bansal, B.K., 2013. Estimation of strong ground motion from a great earthquake in central seismic gap region using empirical green's function method. PAGEOPH. http://dx.doi.org/10.1007/s00024-013-0647-0.
Sharma, B., Chingtham, P., Sutar, A.K., Chopra, S., Shukla, H.P., 2015. Frequency dependent attenuation of seismic waves for Delhi and surrounding area, India. Ann. Geophys. 58 (2). http://dx.doi.org/10.4401/ag-6636.
Sharma, B., Chopra, S., Kumar, V., 2016. Simulation of strong ground motion for 1905 Kangra earthquake and a possible mega thrust earthquake (Mw 8.5) in western Himalaya (India) using Empirical Green's Function technique. Nat. Hazards 80 (1), 487–503.
Sharma, B., Rastogi, B.K., 2014. Spatial distribution of scatterers in the crust of Kachchh region, Western India by inversion analysis of coda envelopes. Disaster Adv. 7 (5), 84–93.
Sharma, B., 2014. A comparative attenuation study of seismic waves in terms of seismic Albedo for Chamoli, Kachchh and Koyna regions of India. Int. J. Eng. Sci. Invent. 3 (6), 33–40.
Sinha, R., Tandon, S.K., Gibling, M.R., Bhattacharjee, P.S., Dasgupta, A.S., 2005. Late Quaternary geology and alluvial stratigraphy of the Ganga basin. J. Himalayan Geol. 26, 223–240.
Su, F., Anderson, J.G., Zeng, Y., 2006. Characteristics of ground motion response spectra from recent large earthquakes and their comparison with IEEE standard 693. In: Proceedings of 100th Anniversary Earthquake Conference, Commemorating the 1906 San Francisco Earthquake. San Francisco, California; April 18–22.
Wang, Z., Zhao, D., Mishra, O.P., Yamada, A., 2006. Structural heterogeneity and its implications for the low frequency tremors in southwest Japan. Earth Planet. Sci. Lett. 251, 66–78.
Wang, K., Fialko, Y., 2015. Slip model of the 2015 M_W 7.8 Gorkha (Nepal) earthquake from inversions of ALOS-2 and GPS data. Geophys. Res. Lett. 42, 7452–7458. http://dx.doi.org/10.1002/2015GL065201.
Yagi, Y., Okuwaki, R., 2015. Integrated seismic source model of the 2015 Gorkha, Nepal, earthquake. Geophys. Res. Lett. 42, 6229–6235. http://dx.doi.org/10.1002/2015GL064995.
Zhao, W., Nelson, K.D., Che, J., Quo, J., Lu, D., Wu, C., Liu, X., 1993. Deep seismic reflection evidence for continental underthrusting beneath southern Tibet. Nature 366, 555–559.